Hemichannel and Junctional Properties of Connexin 50

Derek L. Beahm and James E. Hall
Department of Physiology and Biophysics, University of California, Irvine, California 92697-4560 USA

ABSTRACT Lens fiber connexins, cx50 and cx46 (α3 and α8), belong to a small subset of connexins that can form functional hemichannels in nonjunctional membranes. Knockout of either cx50 or cx46 results in a cataract, so the properties of both connexins are likely essential for proper physiological functioning of the lens. Although portions of the sequences of these two connexins are nearly identical, their hemichannel properties are quite different. Cx50 hemichannels are much more sensitive to extracellular acidification than cx46 hemichannels and differ from cx46 hemichannels both in steady-state and kinetic properties. Comparison of the two branches of the cx50 hemichannel *G-V* curve with the junctional *G-V* curve suggests that cx50 gap junctions gate with positive relative polarity. The histidine-modifying reagent, diethyl pyrocarbonate, reversibly blocks cx50 hemichannel currents but not cx46 hemichannel currents. Because cx46 and cx50 have very similar amino acid sequences, one might expect that replacing the two histidines unique to the third transmembrane region of cx50 with the corresponding cx46 residues would produce mutants more closely resembling cx46. In fact this does not happen. Instead the mutant cx50H161N does not form detectable hemichannels but forms gap junctions indistinguishable from wild type. Cx50H176Q is oocyte lethal, and the double mutant, cx50H61N/H176Q, neither forms hemichannels nor kills oocytes.

INTRODUCTION

Both the lens fiber cell connexins, cx46 and cx50, form functional hemichannels when exogenously expressed in *Xenopus laevis* oocytes (Ebihara and Steiner, 1993; Gupta et al., 1994; Ebihara et al., 1995; Zampighi et al., 1999). Moreover knockouts of either of these connexins separately result in congenital cataracts (Gong et al., 1997; White et al., 1998). Because neither connexin alone can maintain a normal transparent lens, either the conductance of one connexin alone is insufficient or the two connexin types each bring unique essential properties to the lens.

Although the properties of cx46-induced currents have been extensively studied in *Xenopus laevis* oocytes at both the macroscopic and single channel levels (Pfahnl and Dahl, 1999; Ebihara et al., 1995; Ebihara and Steiner, 1993), little is known about the properties of cx50 hemichannels. Preliminary observations of the properties of cx50 hemichannels have been reported by Zampighi et al. (1999), but the primary focus of their paper was morphological. This study focuses on the electrophysiological properties of cx50 hemichannels expressed in *Xenopus laevis* oocytes and reports the effects of voltage, external pH, and external calcium. We show that cx50 hemichannels differ dramatically from cx46 hemichannels in their voltage gating and sensitivity to external pH but not in their sensitivity to external calcium concentration. Because both voltage and pH vary throughout the lens, these differences in hemichannel properties, as distinct from their junctional properties, may be relevant to lens physiology. Moreover the "leak" channels responsible for observed sodium and potassium permeabilities in fiber cell membranes remain unidentified, and it is conceivable, although far from certain, that connexin hemichannels may contribute to these conductances (Eckert et al., 1998).

There is some precedence for using hemichannel properties to elucidate the nature of junctional gating but not always successfully. Ebihara et al. (1995) compared the voltage dependence of cx46 and cx56 hemichannels with the corresponding voltage dependence of junctional conductances. On the basis of the properties of the negative branch of the hemichannel *G-V* curve alone, they assigned a relatively negative gating polarity to the junctional conductances. But single channel measurements demonstrated later that cx46 actually gates with relatively positive polarity (Trexler et al., 1996). The difficulty with the first study was the inability to resolve that portion of the positive *G-V* curve that leads to channel closure. Thus, an appropriate discrimination between the two gates could not be made. Two quite different voltage gates of opposite polarities are resolvable in cx50 macroscopic hemichannel currents. By comparing the voltage gating of cx50 hemichannels and cx50 gap junctions, we show that the cx50 gap junction channel gating is accurately predicted by the gating behavior of cx50 hemichannels at positive potentials and not negative potentials. Thus, we establish definitively that cx50 gap junction gating is relatively positive.

Both cx46 and cx50 hemichannels open when external calcium is reduced and close upon cytosolic acidification. Although cx46 hemichannels are relatively insensitive to acidic external pH (Jedamzik et al., 2000), we show that cx50 hemichannels are almost completely closed by mildly acidic external pH. One of the most striking differences between cx50 and cx46 is the presence of two histidines in the third transmembrane segment of cx50 substituting for asparagine and glutamine in cx46. One

Submitted October 9, 2001, and accepted for publication December 26, 2001.

Address reprint requests to James E. Hall, Department of Physiology and Biophysics, University of California, Irvine, CA 92697-4560. Tel.: 949-824-5835; Fax: 949-824-3143; E-mail: jhall@uci.edu.

© 2002 by the Biophysical Society

0006-3495/02/04/2016/16 $2.00

consequence of this is sensitivity of cx50 hemichannel currents to the histidine-modifying reagent diethylpyrocarbonate (DEPC) and a lack of DEPC sensitivity of cx46 hemichannel currents. In an attempt to determine if some of the differences in the properties of cx46 and cx50 hemichannels resided in these histidines, we engineered the corresponding amino acids of cx46 into the cx50 histidine sites. Although our data did not confirm or rule out a contribution of the unique histidine residues in the third transmembrane domain of cx50 to its increased pH sensitivity over cx46, they did demonstrate that these histidines play a crucial role in the ability of cx50 to form hemichannels. One of these mutations eliminated hemichannel currents without altering the voltage-dependent behavior of gap junction channels formed by the mutant connexin. This result provides us with an opportunity to examine in vivo the separate contributions that hemichannels and gap junction channels make in lens physiology.

MATERIALS AND METHODS

In vitro transcription

Cx46 and cx50, previously subcloned into the SP64T transcription vector, were a kind gift of David Paul (Harvard). Constructs were linearized with restriction endonucleases, and capped mRNAs were transcribed in vitro with SP6 RNA polymerase using the mMessage mMachine kit (Ambion Inc., Austin, TX) according to the manufacturer's instructions. Purity and yield of transcribed mRNA were assessed by agarose gel electrophoresis. Ethidium bromide staining intensity was compared with a known standard to assess yield. Connexin mRNAs were stored as 1 μg/μL master stocks at -80°C.

Working stocks were prepared by serial dilution of the master stock into RNAse-free water and also stored at -80°C. Unlike cx46 mRNA stocks, cx50 mRNA stocks appeared to become more effective per weight of RNA injected with repeated freeze-thaw cycles as indicated by inducing larger hemichannel currents with each use. This held true for different stocks prepared from different transcription reactions and could not be attributed to differences in oocyte translation capacity because cx46 mRNA produced consistent currents. Gel analysis demonstrated no degradation of RNA with freeze-thaw cycles, and we saw channels with the same functional properties regardless of whether or not the RNA had been frozen zero times or multiple times.

Oocyte preparation

Ovarian lobe tissue containing oocytes in all stages of development was surgically removed from adult female *Xenopus laevis* (obtained from the following suppliers: *Xenopus* I, Ann Arbor, MI; NASCO, Ft. Atkinson, WI; or Pacific Biological, Sherman Oaks, CA) anesthetized in 0.3% tricaine chilled to 4°C to 6°C. The tissue was teased apart into smaller clumps containing 6 to 12 oocytes and incubated on a rotating platform at 17°C for 1 h in Ca^{2+}-free ND96 containing 1.5 mg/ml collagenase and trypsin inhibitor. After washing with Ca^{2+}-free ND96, stage V-VI oocytes were selected from the population, manually defolliculated if necessary, and incubated at 17°C for 24 h in ND96 supplemented with 25 mM sodium pyruvate and either 0.05 mg/ml gentamicin or penicillin-streptomycin. Oocytes were injected with 3 to 5 ng of cx38 antisense RNA that suppresses endogenous gap junction expression (Barrio et al., 1991; Hennemann et al., 1992; Bruzzone et al., 1993). Oocytes were injected with 23 to 46 nL of cRNA (Ambion kit) coding for either cx46 or cx50 from stock concentrations ranging from 0.5 μg/μL to 0.0005 μg/μL and then incubated as above but in the presence of 1 mM $CoCl_2$ to reduce hemichannel steady-state conductance. Voltage clamp experiments began 18 to 48 h after cRNA injections.

ND96 contained 96 mM NaCl, 2 mM KCl, 1.8 mM $CaCl_2$, 10 mM HEPES, pH 7.4. Ca^{2+}-free ND96 consisted of ND96 with no added calcium. Different calcium concentrations were achieved by adding calcium to this solution from a 1 M stock. The osmolarity of all solutions, measured using a Vapor Pressure Osmometer (Wescor Inc., Logan, UT) was 200 to 210 mmol/kg. In experiments where pH was varied ND96 was prepared using buffers appropriate to the particular pH range (pH 6.0–6.7, PIPES; pH 7.3–8.2, HEPES; pH 8.7–9.7 CHES).

Pairing oocytes for gap junction formation experiments

Oocytes were transferred to petri dishes coated with 2% agaraose 24 to 72 h after cRNA injections for removal of the vitelline layer before pairing. The vitelline layer was separated from the plasma membrane by incubation in hypertonic solution (up to 2 × ND96) and then manually removed with no. 5 Dummont forceps. Variations of calcium concentration and osmolarity of the stripping solution did not affect the experimental results. Before pairing, devitellinized oocytes were incubated for 20 to 30 min in ND96 supplemented with 1 mM $CoCl_2$ to prevent spontaneous hemichannel activity and consequent diminution of oocyte viability.

Electrophysiology

Voltage clamp recordings of macroscopic membrane currents were obtained using a two-electrode voltage clamp. AxoClamp 2B and 2A voltage clamps (Axon Instruments, Inc., Foster City, CA) using a 1 × L headstage for voltage recording and a 10 × MG headstage for passing current were used in one or two oocyte configurations. The bath potential was clamped to 0 mV using a 100 × VG headstage. Voltage recording and current passing electrodes were pulled from borosilicate glass on a horizontal puller (Flaming-Brown P-87, Sutter Instruments, Novato, CA). The internal pipette solution consisted of 150 mM KCl, 10 mM EGTA, 10 mM Hepes, pH 7.2 to 7.4. Voltage-recording electrodes had resistances between 1 and 3 MΩ. Current passing electrodes had resistances of 0.1 to 0.3 MΩ with a 1-mm agarose bridge at the tip to prevent leakage of KCl into the oocyte. Command pulses and current measurements were generated using Pclamp 6.0 data acquisition software (Clampex 6.0) to control the amplifiers interfaced to a PC through a Digidata 1200 A/D converter. Currents were filtered at 50 to 200 Hz and acquired directly to hard drive.

After pairing for a minimum of 2 h, the oocytes were clamped to a potential equal to the average of the two resting potentials using dual two-electrode-voltage-clamps (Axoclamp 2A and 2B amplifiers, Axon Instruments). Hemichannel currents and gap junctional currents were recorded at various times and during perfusions with various solutions. Ten to 15 times the bath volume was sufficient to fully exchange bath medium. At the end of each experiment, the membrane potentials of oocytes were recorded under the original bath conditions to assess viability of the oocytes.

RESULTS

Properties of cx46 and cx50 expressed in *Xenopus* oocytes

We screened for heterologously expressed functional hemichannels by measuring magnitude and voltage dependence of whole-cell currents of connexin-cRNA-injected

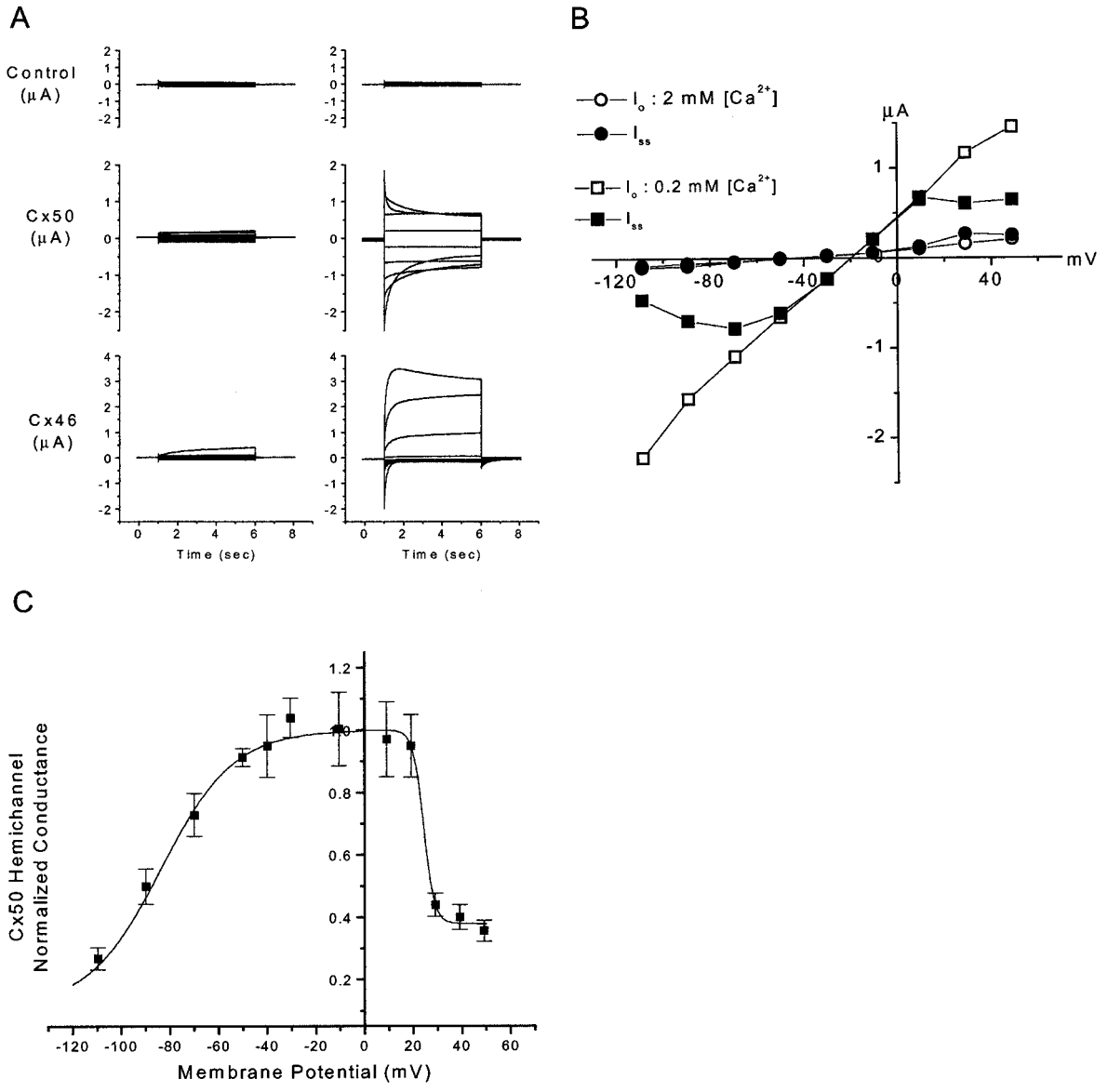

FIGURE 1 Functional expression of cx46 and cx50 hemichannels in single *Xenopus* oocytes. (*A*) Current voltage families of whole-cell currents in single *Xenopus* oocytes. In each case five-second voltage steps from −110 mV to +50 mV in 20 mV increments were applied from a holding potential of −20 mV. Currents were recorded 48 h after injecting stage VI oocytes with 23 nL of RNAse-free water containing no RNA (*top panel*), 20 ng of mouse cx50 cRNA (*middle panel*), or 0.1 ng of rat cx46 cRNA (*bottom panel*). Decreasing $[Ca^{2+}]_{out}$ from 2.0 mM (*left*) to 0.2 mM (*right*) increased the amplitude of whole-cell currents elicited in cx46 and cx50 cRNA-injected oocytes but not in water-injected control oocytes. Bath solution was standard ND96 at pH 7.4. (*B*) Initial and steady-state current-voltage relationship for cx50 hemichannels. Initial currents and steady-state currents were determined by fitting current traces to a single or double exponential between 0.02 and 5 s. Initial (*open symbols*) and steady-state (*solid symbols*) currents were plotted against membrane potential for $[Ca^{2+}]_{out}$ of 2.0 mM (*circles*) or 0.2 mM (*squares*). (*C*) Normalized *G-V* relationship for cx50 hemichannels generated by dividing steady-state hemichannel conductance at each voltage by the initial conductance determined from the slope of the initial I-V curve shown in *B*. The solid line is the Boltzmann fit, determined separately for positive and negative voltages. Curve-fitting parameters are listed in Table 1.

oocytes in the presence and absence of external calcium. Fig. 1 compares the typical calcium-sensitive currents that develop in *Xenopus laevis* oocytes injected with cRNA coding for rat cx46 and mouse cx50 with currents in uninjected oocytes. In Fig. 1 *A* we compare the effects of lowering the Ca^{2+} concentration from 2 to 0.2 mM on uninjected oocytes, oocytes injected with cx50 RNA (20 ng), and oocytes injected with cx46 RNA (0.1 ng). The same pulse protocols were used for each case (see figure legend for details). Cx50 currents have very different voltage dependence from those of cx46, results reported earlier by Zampighi et al. (1999) for cx50 and by Ebihara et al. (Paul et al., 1991) for cx46. Qualitatively Zampighi et al.'s Ca^{2+} dependence is similar, but with subtle differences to

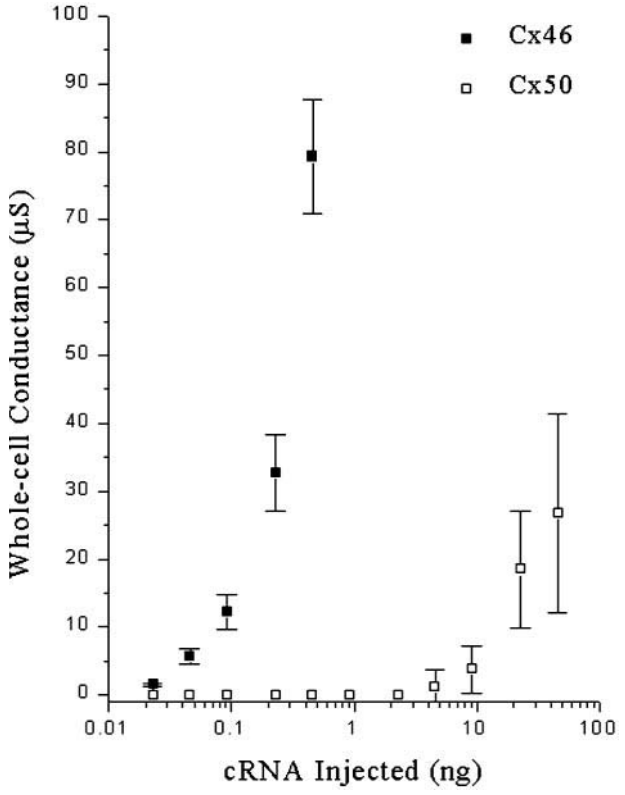

FIGURE 2 RNA-dose dependence of cx46 and cx50 hemichannel expression. Oocytes were injected with 46 nL of RNAse-free water containing various amounts of cRNA prepared from serial dilutions of 1 μg/μL stocks. Stock concentrations were estimated by comparison to known quantities of standards ran in parallel on 0.8% TEA gels and stained with ethidium bromide. Two days after injection, oocytes were voltage clamped to either −20 mV (cx50) or −10 mV (cx46) in ND96 supplemented with 1mM $CoCl_2$. Whole-cell conductance was determined as the change in current induced by a 20-mV voltage pulse applied before and after equilibrating oocytes in 0.1 mM $CaCl_2$, pH 7.4, ND96 for 5 min. The difference in whole-cell conductance was plotted as a function of injected cRNA amount. Cx46 (■) and cx50 (□). Each data point is the mean value and standard deviation of measurements made in three to five oocytes.

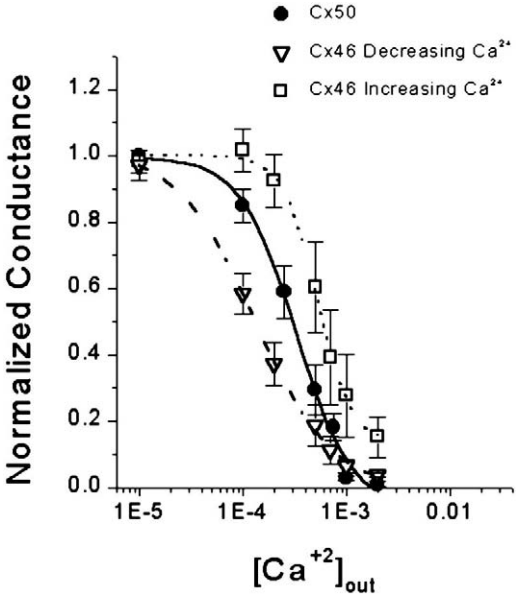

FIGURE 3 Dependence of cx46 and cx50 hemichannel currents on external calcium. Voltage steps of 5-s duration were applied in 20 mV increments between −100 and +20 mV from a holding potential of −20 mV (cx50) or −10 mV (cx46). Slope conductance was determined from the linear region of the I-V curve generated by plotting the initial current amplitude (resolved at 30 ms) as a function of membrane potential. Voltage steps were applied 2 to 3 min after completely exchanging the media with 10 to 15 bath volumes of ND96 containing different calcium concentrations. The slope conductance obtained for each calcium concentration was normalized to the slope conductance obtained in ~0.010 mM (0 added calcium ND96). Data are expressed as the mean and standard deviation of measurements obtained from three different oocytes for cx50 and five oocytes for cx46 and plotted against the log $[Ca^{2+}]_{out}$. Cx50 (●), cx46 decreasing $[Ca^{2+}]_{out}$ (△), and cx46 increasing $[Ca^{2+}]_{out}$ (□).

be discussed later. Fig. 1, *B* and *C*, shows the strong voltage dependence of cx50 hemichannels. Crucially we show here for the first time that the voltage dependence of the positive and negative branches of the *G-V* curve differ greatly in steepness. The Boltzmann parameters of the positive and negative branches are very different and can be used to determine the relative polarity of cx50 junctional voltage gating.

Finally, Fig. 2 shows that the expression levels of cx50 and cx46 for a given quantity of injected cRNA are quite different. Comparative cRNA dose-response curves for hemichannel currents induced in a single batch of oocytes are shown in Fig. 2. Cx50 required 2 to 3 orders of magnitude more cRNA than cx46 to generate similar whole-cell conductances under the usual conditions of pH (pH 7.4) and calcium, but as we shall show later, much of this difference results from differences in pH dependence of the cx50 and cx46 conductances.

Both types of hemichannels are blocked by external calcium in a dose-dependent manner with a pK_{Ca} of ~200 μM (Fig. 3). We found that Ca^{2+} did not shift the *G-V* curve or alter the kinetics of cx50 hemichannels, a result quite different from that found by Ebihara and Steiner (1993) for cx46 hemichannels. Although cx50 and cx46 both have essentially the same sensitivity to Ca^{2+}, the response of cx46 exhibits considerable hysteresis, whereas that of cx50 does not. As both sets of data were obtained under nearly the same conditions, these results are consistent with the difference in the kinetics of Ca^{2+} action on the two proteins. A less quantitative dependence of cx50 hemichannel conductance on Ca^{2+} was reported earlier by Zampighi et al. (1999). They measured steady-state current at −50 mV as a function of external calcium, but the data in Fig. 3 show conductance of the linear part of the I-V curve as a function of calcium concentration. Oocytes exposed to calcium concentrations below 1 to 10 μM often developed a large nonspecific leak conductance that persists after readdition of

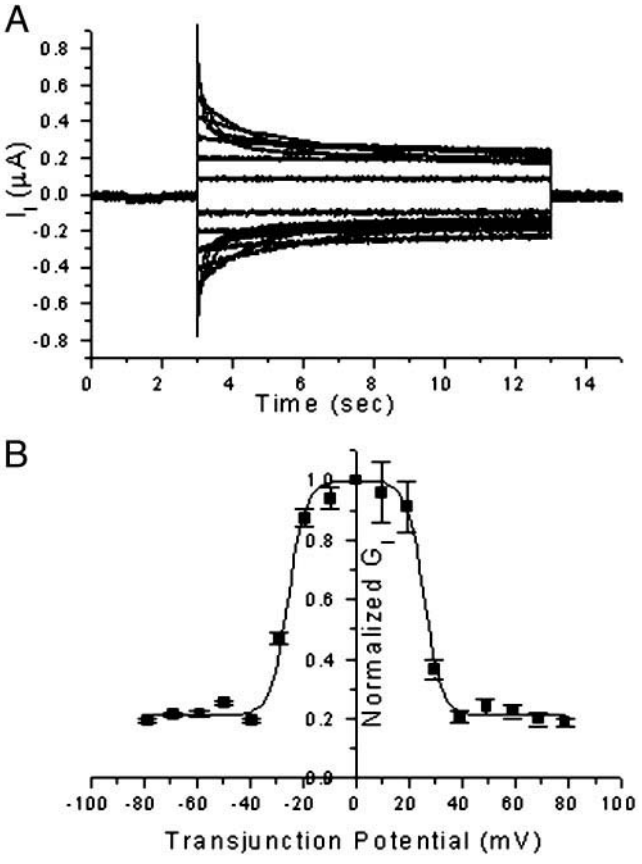

FIGURE 4 Voltage dependence of cx50 gap junction channels. Cx50 cRNA-injected oocytes were stripped of their vitelline layers and paired for 4 to 24 h before voltage clamping in a dual-two-electrode voltage clamp configuration. Both oocytes were clamped to −40 mV in ND96 supplemented with 1 mM $CoCl_2$. Junctional currents (*A*) were elicited by imposing transjunctional potentials ranging from ±10 mV to ±80 mV in 10-mV increments. Initial and steady-state current amplitudes were obtained by fitting the current trace between 20 ms and 10 s to the sum of two exponentials and extrapolating to time = 0 or infinity, respectively. Initial and steady-state conductances were normalized to their values at ±10 mV and plotted against the transjunctional potential (*B*). Data were fit to a Boltzmann equation (*smooth line*) with the parameters listed in Table 1.

calcium. Therefore, very low calcium concentrations were avoided.

Comparing hemichannels to gap junction channels

Cx50 homotypic gap junctional currents are shown in Fig. 4. Only oocyte pairs with maximum junctional conductances less than 10 μs were used to examine the voltage dependence of junctional currents. For larger conductances, access resistance becomes significant and produces an apparent reduction in voltage sensitivity (Jongsma et al., 1991; Wilders and Jongsma, 1992).

The normalized steady-state conductance was fit to a Boltzmann distribution of the usual form: $G_{jss} = (G_{jmax} - G_{jmin})/(1 + \exp(A(V - V_0))) + G_{jmin}$, in which G_{jss} is the steady-state conductance normalized to its value at ±10 mV, G_{jmax} and G_{jmin} are the maximum (usually 1.0) and minimum normalized conductances, A is the cooperativity constant, and V_0 is the voltage at which G_{jss} is one-half maximal or $(G_{jmax} + G_{jmin})/2$. The cooperativity constant can also be expressed as an apparent gating charge n, in which $n = A(kT/q)$ with k as the Boltzmann constant, T as the absolute temperature, and q as the elementary charge (Hille, 1992). These parameters for cx50 gap junction channels, cx46 hemichannels, and gap junctions are presented in Table 1.

Fig. 5 compares the voltage dependence of cx50 gap junctional conductance with the voltage dependence of nonjunctional hemichannel gates. Fig. 5 *C* clearly shows that cx50 hemichannels have two distinct gates with different properties, the voltage dependence of the positive gate being much steeper than that of the negative gate. Cx50 gap junctions, of course, have a symmetric *G-V* curve that manifests only one polarity and one voltage sensitivity (Fig. 4 *B*; Zampighi et al., 1999). The steeper voltage sensitivity of cx50 hemichannels at positive potentials is almost exactly twofold greater than that of cx50 gap junction channels. This result is expected if exactly one-half of the transjunctional voltage drops across each hemichannel of a gap junction channel. Under this assumption, the voltage

TABLE 1 Boltzmann parameters describing the *G-V* relationship of hemichannels and gap junction channels formed from lens fiber cell connexins

Protein	Channel type	$A(mV^{-1})$	n	V_o(mV)	G_{jmin}/G_{jmax}
cx50	Junction	0.30 ± 0.02		25.6 ± 0.4	0.21 ± 0.01
cx50H161N	Junction	0.29 ± 0.02		25.9 ± 1.2	0.23 ± 0.05
cx46	Junction	0.08 ± 0.02		59 ± 4.7	0.05 ± 0.04
cx38	Junction	0.13	3.3	35	0.35
cx50*	Junction	0.34	8.5	18	0.14
cs46*	Junction	0.09	2.2	67	0.10
cx50	Hemichannel (positive V)	0.54 ± 0.11	16.7	25.0 ± 0.11	0.36 ± 0.02
cx50	Hemichannel (negative V)	0.06 ± 0.01		−82.6 ± 4.6	0.11 ± 0.12

*Cx46 and cx50 homotypic channel data are from (White et al., 1994b). $n = A(kT/q)$ and at 20°C (kT/q) = 25.3 mV. Other data are from the present work.

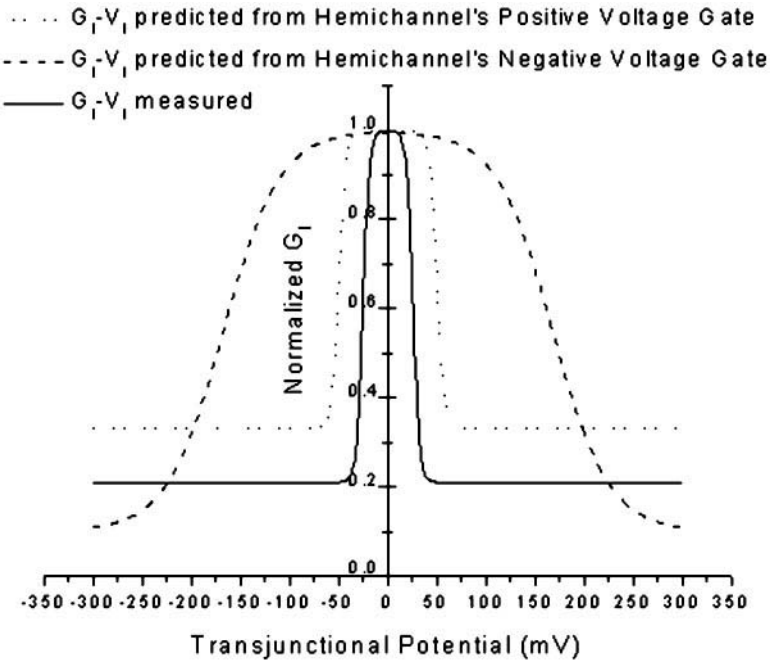

FIGURE 5 Comparison of the G_j-V_j relationship of cx50 gap junction channels with the *G-V* relationship of cx50 hemichannels at positive and negative voltages. The steady-state G_j-V_j curve of cx50 homotypic gap junctions (*solid line*) is compared with the predicted steady-state G_j-V_j curves calculated from hemichannel current data at positive (*dash*) and negative (*dot*) voltages. The steady-state G_j-V_j curve predicted from hemichannel current data was determined by using the Boltzmann parameters to generate a simulated curve as a function of $V_j/2$. The Boltzmann parameters describing the normalized steady-state *G-V* curve of hemichannel conductance (Fig. 1) were used to estimate the steady-state current in a gap junction channel. Assuming that the voltage-dependent open probabilities of the two opposing hemichannels are symmetric ~0 mV, the predicted steady-state G_j-V_j is calculated as $G_{j,ss} = [P_{ss}, A(V_j/2) \times P_{ss}, B(V_j/2)]/[P_{ss}, A(0) \times P_{ss}, B(0)]$ Steady-state G_j-V_j curves are predicted separately for the positive (*dashed*) and negative (points) voltage gates of the hemichannel.

sensitivity of the positive gap-junctional gate examined in nonjunctional membranes in the hemichannel configuration would appear twofold greater than its sensitivity in a complete gap junction.

The cx50 hemichannel I-V curve suggests that only one type of voltage gate (the more voltage-sensitive one) is active in junctional gating, and positive voltages close that gate. Two arguments can be made that this is the case. The first and most convincing argument is that the steepness of the junctional *G-V* curve is accurately predicted by the steepness of the positive branch of the hemichannel *G-V* curve. The second is that the V_0 of the positive branch of the hemichannel *G-V* curve is less than that of the negative branch. Thus, even if both polarities of hemichannel gate remained functional in the junctional configuration, only the positive gate would be seen because one of the two opposed positive gates would close before either of the less sensitive opposed negative gates.

Macroscopic conductance of cx50 hemichannels, but not cx46 hemichannels, is highly pH sensitive

Because pH may play an essential role in lens physiology (Bassnett and Duncan, 1988; Pasquale et al., 1990; Mathias et al., 1991; Miller et al., 1992), we examined cx46 and cx50 hemichannel currents for sensitivity to external pH. Fig. 6, *A* and *B*, show representative cx46 and cx50 hemichannel currents at different external pH values. Zampighi et al. (1999) reported that lowering internal pH with sodium acetate in the bathing buffer reduces conductance of cx50 hemichannels expressed in oocytes, but ours is the first report of effects of external pH on cx50 hemichannels. The response of cx46 hemichannels to pH has been studied by Trexler et al. (1996) who found acidification closed cx46 hemichannels on a titration curve with a pK of 6.4 and an apparent Hill coefficient of 2.3. Our observations of the pH dependence of cx46 are consistent with theirs, although we find that conductance of cx46 is less reduced at pH 6.7 than current at a fixed voltage, the data used by Trexler et al. (1996). Whereas the sensitivity of cx46 hemichannels to external pH varies between different batches of oocytes, changes in extracellular pH exert only a minor effect on cx46 whole-cell currents above pH 6.7. Even when oocytes expressing cx46 are clamped at potentials more positive than −10 mV to maintain a large percentage of hemichannels in the open state, whole-cell conductance is reduced by no more than 30% when the external pH is decreased from 7.6 to 6.2 (data not shown).

In contrast, cx50 hemichannel currents are very sensitive to external pH and are undetectable when the pH is lower than 6.5. In fact, the macroscopic conductance of cx50 hemichannels at pH 7.0 is only approximately one-third of that at pH 7.7. Fig. 6 *C* is a plot of the slope conductance of cx50 hemichannels against pH measured in the linear region of the I-V curve between −30 and +20 mV. The effect of lowering external pH is very rapid and occurs immediately on perfusion of low pH solutions. This suggests, but certainly does not prove, that the site of proton action is external. But our data do not rule out an internal site of proton action. Neither Ca^{2+} concentration nor holding potential alters the shape or position of this curve (data not shown). The titration curve in Fig. 6 *C* shows evidence for two different sites of proton action, but the data do not extend to high enough pH to fully characterize the more

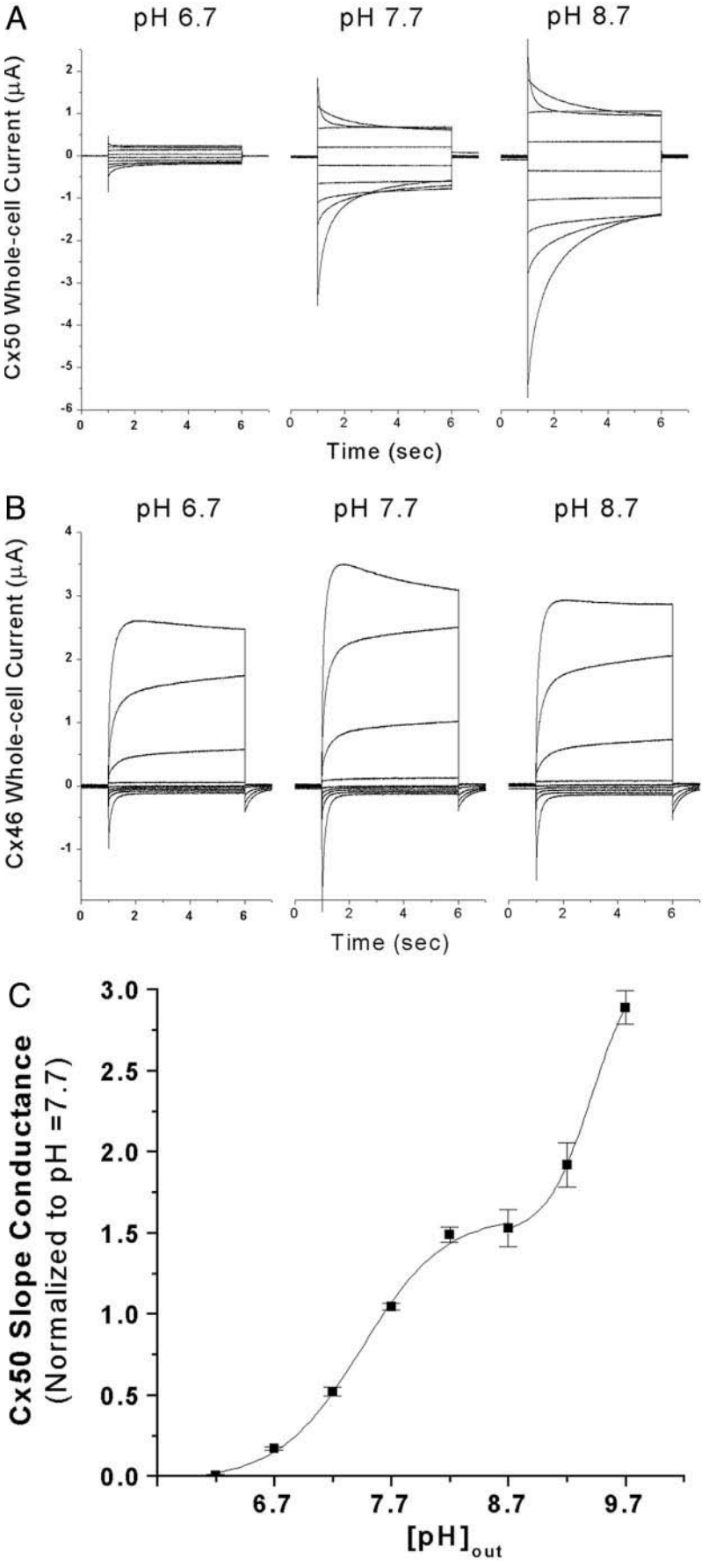

FIGURE 6 Cx50 hemichannel currents are very sensitive to external pH. Examples of hemichannel currents recorded in cx50 (*A*) and cx46 (*B*) cRNA-injected oocytes equilibrated for 3 to 5 min in a series of modified ND96 solutions. Each family of current traces was elicited by applying 5-s voltage steps of −110 mV to +50 mV in 20-mV increments from a holding potential of −20 mV with an interepisode time of 30 s. (*C*) For oocytes expressing cx50 hemichannels, the slope conductance at different pH values was obtained from a linear fit of the initial I-V relationship and then normalized to the slope conductance measured at pH 7.7. The normalized slope conductances were plotted against pH to generate a proton dose-response curve. Data points and error bars represent the mean and standard deviation of measurements in six different oocytes. Cx50 hemichannels showed a biphasic response to external pH. Conductance increased sigmoidally between pH 6.2 and 8.7. This portion of the curve (when treated independently) was well fit by a Hill equation (Hill coefficient = 0.62 ± 0.10) yielding one-half-maximal conductance at pH 7.42. Conductance began to increase again at pH values greater than 8.7, but a second maximum could not be determined due to irreversible increases in whole-cell leak conductance at pH values greater than 9.7. A nonbuffered ND96 stock solution containing 0.2 mM $CaCl_2$ was used to prepare all solutions. The following buffers were used at 10 mM to achieve the different pH values (PIPES, pH 6.0–6.7; HEPES, pH 7.3–8.2; CHES, pH 8.7–9.7)

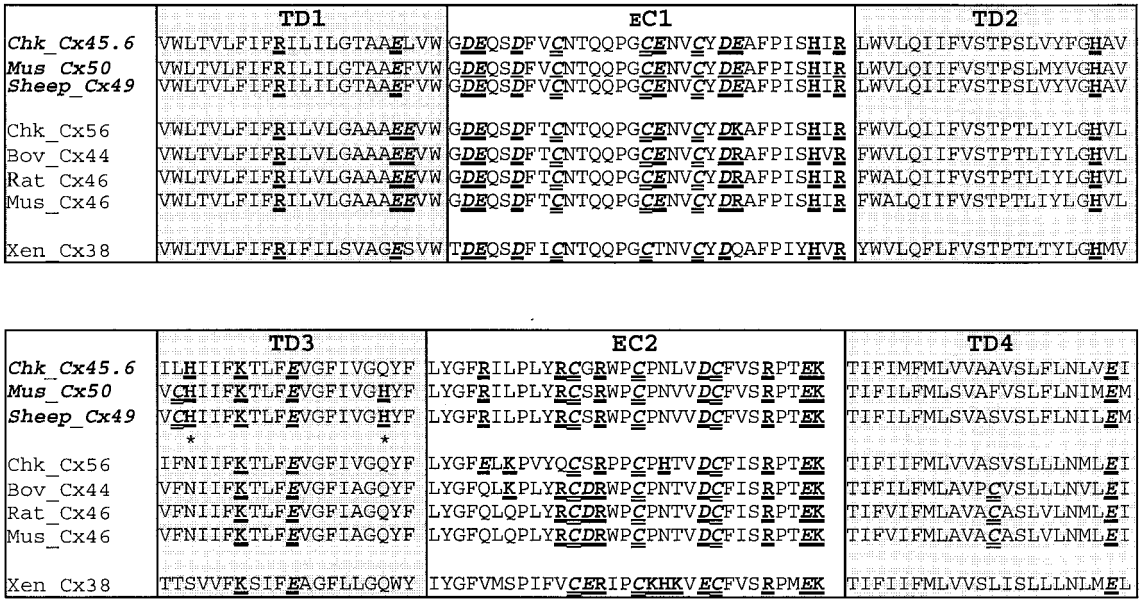

FIGURE 7 Connexin residues potentially exposed to extracellular environment. Amino acid residues that are potentially exposed to the extracellular environment are shown for connexins (and their homologues) known to form functional hemichannels in *Xenopus* oocytes. Sequences were aligned and divided into transmembrane domains. Basic residues are shown bold and underlined (e.g., **K**), acidic residues are shown bold, italic, and underlined (e.g., ***E***), histidines are shown in outline type underlined (e.g., +), and cysteines are shown bold and double underlined (**C**).

alkaline site. Fitting only the lower part of the curve to the Hill equation gives a pK of 7.42 and an apparent Hill coefficient of ~0.6.

Unique histidine residues are located in the presumptive pore of cx50

Sequence comparison of hemichannel-forming connexins reveals two histidine residues unique to the presumptive third transmembrane domain of cx50. These might play a role in conferring unique on properties cx50 hemichannel currents. (Goodenough et al., 1988; Milks et al., 1988; Laird and Revel, 1990; Yeager and Gilula, 1992). Fig. 7 compares amino acid sequences of the two extracellular loops and the four transmembrane domains of rat cx46, mouse cx50, and their homologues cloned from other species. These domains, together with the N-terminal domain, represent the most conserved regions shared by all connexins cloned to date. The amphipathic nature of the third transmembrane domain, TD3, suggests that it could line the pore of gap junction channels. However, cysteine-scanning mutagenesis shows that both TD1 and TD3 contribute pore-lining residues (Pfahnl and Dahl, 1998). Both cx50 H161 and H176 occupy positions in TD3 and therefore could line the pore and confer unique properties on cx50. These two histidine residues are replaced by uncharged polar amino acids at equivalent positions in most other connexins including cx46.

DEPC modification of histidine residues completely blocks cx50 current

We tested if modification of externally accessible histidine residues could influence hemichannel activity by treating oocytes with diethyl pyrocarbonate (DEPC). DEPC reacts with exposed histidine, tyrosine, and sulfhydryl residues, but preferentially modifies histidine residues at pH 6.0 in which reactivity with nonhistidine residues is minimal (for example, see Padan et al., 1979; Miles, 1977; Rai and Wolff, 1998). Furthermore, exposure to hydroxylamine specifically reverses only the modification of histidine residues, thereby providing an internal control against artifacts that could arise from DEPC modification of nonhistidine residues (Shoshan-Barmatz and Weil, 1994). DEPC is very hydrophilic, and one would expect that it could not cross-biological membranes readily. This contention was experimentally verified by Spires and Begensich (1990) who showed that relatively low concentrations of external DEPC (20–500 μM) slowed the opening of potassium channels in squid giant axons but that internal DEPC at 2 mM had no effect. Fig. 8 shows that a 30-s treatment with micromolar concentrations of DEPC eliminates all cx50 hemichannel current. (DEPC treatment has no effect on cx46 (data not shown).) Oocytes were equilibrated at pH 6.0 before and after the application of DEPC to reduce reaction with other amino acid residues than histidine. Reappearance of cx50 whole cell currents after incubation in 20 mM hydroxylamine clearly demonstrates that modified histidine residues

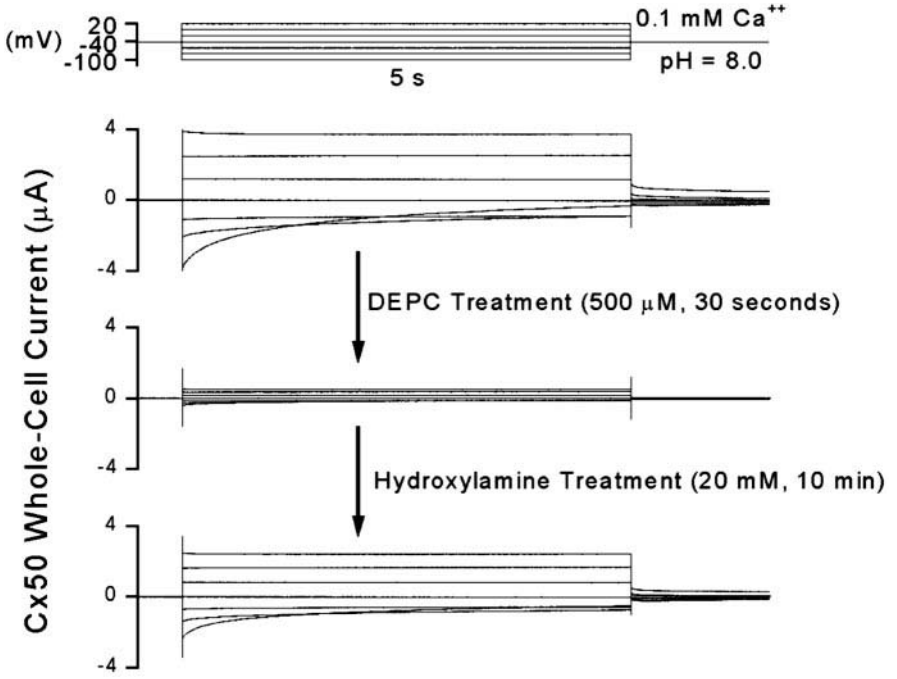

FIGURE 8 Chemical modification of externally accessible histidine residue(s) eliminates cx50 hemichannel currents. Functional expression of cx50 was first verified by whole-cell currents recorded in 0.1 mM Ca^{2+}, pH 8.0 (recording conditions). Oocytes were then perfused with pH 6.0 media for 2 min before and after a 30-s application of freshly prepared 500 μM DEPC solution in pH 6.0 media, and then returned to recording conditions for 3 min before collecting another current family. Oocytes were then incubated for 10 min in 20 mM hydroxylamine (pH 7.4) to reverse DEPC modification of histidines, and then returned to recording conditions for assaying recovered current. Over the course of 1 h, there was no detectable change in the conductance levels of untreated oocytes expressing cx50 or in oocytes treated with DEPC but not hydroxylamine. Control experiments in which oocytes expressing cx50 were not treated with DEPC initially but were incubated with hydroxylamine at pH 7.4 showed currents indistinguishable from those of untreated cx50-expressing oocytes.

mediate this effect. Control experiments demonstrated that hydroxylamine alone had no effect on cx50 hemichannel currents (data not shown). DEPC reactions were performed at pH 6.0, indicating that any histidines modified by DEPC are accessible to external reagents even when the hemichannel is in the closed or blocked configuration induced by low external pH.

Neither voltage nor Ca^{2+} alters the ability of DEPC to modify cx50 hemichannels. Voltages of either -120 mV or $+60$ mV had no effect on the ability of DEPC to modify cx50 hemichannels. This suggests that neither the positive-closing gate nor the negative-closing gate interferes with DEPC access, assuming these voltage-operated gates are unaffected by pH. In experiments where the DEPC modification reaction was carried out in either 2 mM Ca^{2+} or 0 added calcium, the percentage of blocked hemichannel current and the time-dependence of block remained the same. Hence, Ca^{2+} does not alter the ability of DEPC to modify the functional histidines.

Mutational analysis

The cumulative evidence suggests that a histidine residue in the presumptive channel wall of cx50 hemichannels is accessible to externally applied reagents. Although two additional histidine residues are potentially accessible, we focused on the two histidines unique to cx50 because cx46 hemichannels were refractory to modification by DEPC. To investigate the roles of the two histidines in the third transmembrane domain, we constructed mutants in which one or both histidines was replaced with the highly conserved residues found at equivalent positions in cx46. Whole-cell currents in single oocytes injected with cx50H161N were similar to control currents observed in noninjected oocytes. In other words, hemichannel currents were not detectable in oocytes injected with cx50H161N, even with low external calcium and high pH. However, gap junction currents were easily detected 24 h after pairing oocytes (Fig. 9). The presence of gap junctions proves that the absence of detectable hemichannel currents cannot be attributed to improper translation, assembly, or trafficking of the mutant connexin polypeptide to the plasma membrane. Most interestingly, the voltage-dependence and gating kinetics of gap junctions formed by cx50H161N were indistinguishable from those of cx50 wild-type gap junctions. Table 1 includes the $G_j - V_j$ Boltzmann fit parameters for both cx50 and cx50H161N gap junctions. Thus, cx50H161N forms gap junctions that display wild-type voltage-dependent behavior but does not form conductive hemichannels.

The cx50H176Q mutation proved toxic to oocytes. In 8 of 10 batches, oocytes injected with cx50H176Q cRNA followed a pattern of events often ending in lysis. These events were never observed in oocytes from the same batch expressing either wild-type cx46 or cx50 hemichannel currents, and the more mutant RNA injected, the sooner the appearance of deleterious changes in the oocyte. First, disruptions of the pigmentation pattern occurred in the absence of any detectable hemichannel currents. The pigmentation remained confined to the animal cap hemisphere, but an increasing number of small white spots appeared and grew in size over the course of several days (parallel to cx50 wt expression time course). See Fig. 10 *A* for a sketch of an

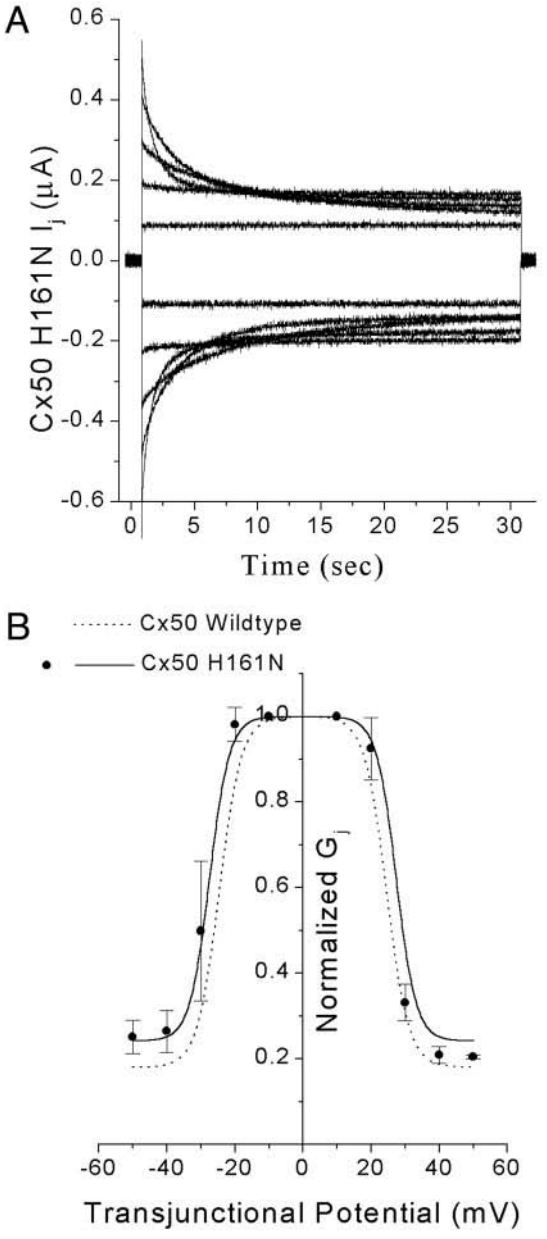

FIGURE 9 Cx50H161N forms gap junctions that are identical to wild-type cx50 gap junctions. (*A*) Junctional currents from pairing cx38 antisense-treated oocytes injected with cx50H161N were elicited by imposing transjunctional voltages from ±10 mV to ±50 mV in 10-mV increments. (*B*) The normalized steady-state G_j-V_j curve was generated as described in Fig. 4 and data were fit to a Boltzmann function (*solid line*) whose parameters were $A = 0.36 = -0.08$, $V_0 = 27.0 \pm 0.8$, and $g_{min} = 0.23 \pm 0.03$, which are practically identical to those determined from cx50 WT as shown in Table 1. The Boltzmann fit from wild-type cx50 data is also shown (*dotted line*) for comparison.

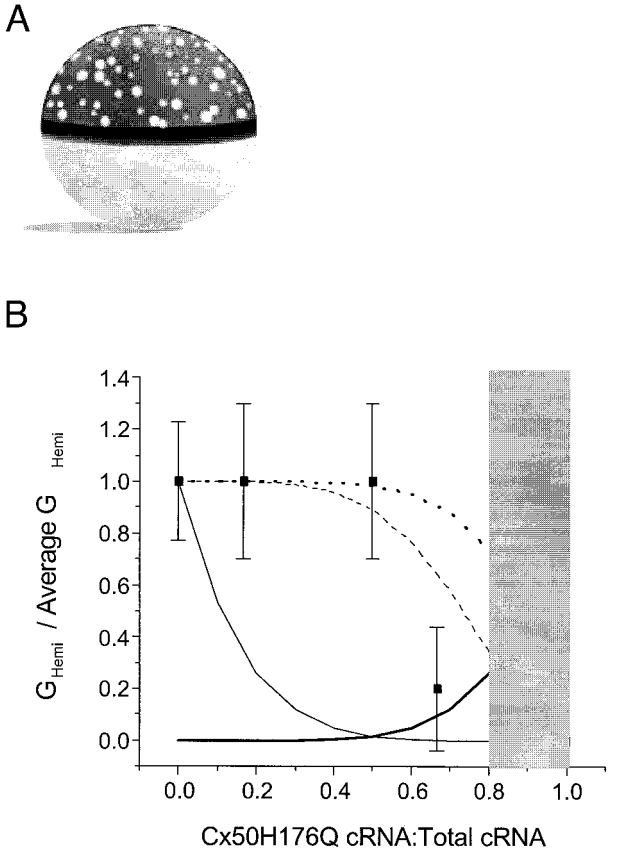

FIGURE 10 cx50H176Q mutant phenotype can be rescued by co-expressing cx50 wild-type cRNA. (*A*) Appearance of oocytes injected with H176Q cRNA after 2 to 3 days. (*B*) Rescue of the cx50H176Q phenotype. Oocytes were injected with 40 ng of total cRNA containing different ratios of cx50H176Q:cx50WT. Hemichannel conductances were assayed in 0.2 mM CaCl2 ND96, pH 8.0 as described in Fig. 1. For each cRNA ratio, the average G_{hemi} was normalized to the average G_{hemi} of oocytes injected with 40 ng of cx50WT. Curves for the expected fraction of hemichannels that are homomeric cx50 WT or homomeric cx50H176Q (*solid lines*), heteromeric hemichannels with a minimum of two WT subunits (*dashed line*), or one WT subunit (*dash-dotted line*) are superimposed on the bar graph. The shaded area represents the cRNA mixes that resulted in oocyte lysis or the spotted pigmentation pattern.

H176Q-injected oocyte. The spots resemble the spots that often develop at the sites of intracellular injections of calcium. Whole-cell currents and resting potentials of oocytes displaying these spotty pigmentation patterns were indistinguishable from those recorded from noninjected control oocytes. Second, at a variable number of days after the first appearance of the white spots, the resting potential of oocytes depolarized to near 0 mV over the course of 4 to 6 h. Depolarization was due to a voltage-independent leak conductance that could not be prevented by incubation in 1 mM Co^{2+} or $pH_{out} < 6.5$ solutions.

To determine if heteromeric hemichannels containing some wild-type (WT) subunits could prevent the lethal phenotype associated with homomeric mutant hemichannels, oocytes were co-injected with WT and mutant cx50H176Q cRNA. Assuming that mutant and wild-type monomers can assemble into the same hemichannel with equal probabilities, the subunit composition of hemichannels formed in oocytes injected with different ratios of mutant to wild-type cRNA can be predicted by the binomial

distribution. The proportion of channels with m mutant subunits, $P(m)$, is determined by the binomial distribution, $P(m) = n!/(m!(n - m)!)(p^{m}(1 - p)^{(n-m)})$, in which p is the fraction of mutant cRNA in the total mix. The total number of subunits that form a single hemichannel is $n = 6$.

Oocytes were injected with ~50 ng of cRNA containing cx50H167Q mutant cRNA and cx50 wild-type cRNA in different ratios. Two days after injection, most of the oocytes receiving high fractions of H167Q cRNA had severely depolarized membrane potentials and large input conductances thereby preventing voltage clamp studies. However, the few remaining oocytes demonstrate that WT cx50 subunits can rescue the H176Q mutant phenotype. Experimental results are shown in Fig. 10 *B*.

The binomial theorem predicts that equal amounts of mutant and WT will generate mainly heteromeric hemichannels, that is channels that have at least one wild-type monomer. Oocytes receiving equal amounts of mutant and WT cRNA had a higher survival rate, lacked white spots in the pigmented animal cap, and expressed the same magnitude of whole-cell hemichannel conductances as oocytes injected with only WT cx50. White spots and a decline in hemichannel current appeared only in oocytes injected with cRNA mixes predicted to generate an increasing population of homomeric mutant hemichannels. These data suggest that this phenotype is rescued by a single WT subunit. However, significantly lower hemichannel conductances were recorded in these oocytes than predicted even if the conductance of homomeric mutant channels were assumed to be zero. Thus, the lower conductance seen at a high proportion of mutant RNA may result from the ability of a single homomeric mutant hemichannel to prevent the trafficking of vesicles containing many functional heteromeric hemichannels. Lowering pH_{out} to 6.3 blocked the hemichannel currents recorded in oocytes expressing all ratios of mutant to wild-type RNA.

DISCUSSION

Introduction

Lens fiber cells express two predominant connexins, cx46 and cx50, which have been shown to form functional hemigap-junction channels in nonjunctional membrane. Cx50 differs dramatically from cx46 in the requirements for inducing detectable hemichannel currents, the voltage dependence, and kinetics of hemichannel gating, and the sensitivity of hemichannel current to external pH. The amount of cRNA required to induce cx50 hemichannel currents under the most commonly used experimental conditions is more than 100-fold greater than that needed to induce cx46 hemichannel currents of comparable magnitude, but if the pH is increased to ~8, the amount of RNA required is only ~30- to 40-fold greater. Moreover less than one-half the available cx50 conductance is seen at neutral pH. Expression levels that produce no detectable currents at pH 7.4 to 7.6 give rise to very large currents at pHs greater than 8.0. Although the unique histidines in the third transmembrane domain of cx50 cannot be shown to contribute to the differences in pH dependence of cx50 hemichannel currents, at least one of them plays an essential role in facilitating hemichannel formation.

This paper thus provides two crucial new results: a cx50 mutant that forms normal junctions but does not form hemichannels and the demonstration that cx50 junctions close with relatively positive potential. We also demonstrate that cx50 hemichannels are more sensitive to acidification of the external medium than cx46 hemichannels. We suggest that these differences in hemichannel properties may be essential to normal lens physiology.

Voltage-dependent properties of Cx50 hemichannels

The voltage dependence and Ca^{2+} sensitivity of cx46 hemichannels expressed in *Xenopus laevis* oocytes have been characterized at both the macroscopic and single channel levels (Ebihara and Steiner, 1993; Trexler et al., 1996; Pfahnl and Dahl, 1998). At the macroscopic level, steady-state whole-cell conductance depends on both $[Ca^{2+}]_{out}$ and voltage. At normal calcium concentrations (>1 mM), oocytes must be depolarized to voltages more positive than −10 mV to activate hemichannel currents. Decreasing $[Ca^{2+}]_{out}$ shifts the cx46 activation curve to more negative potentials (Pfahnl and Dahl, 1998).

The voltage dependence of cx50 hemichannels differs dramatically from that of cx46 hemichannels. The relationship between normalized steady-state hemichannel conductance and membrane potential is shown in Fig. 1 *C*. The steady-state whole-cell hemichannel conductance ($G_{H,\ cx50}$) attains its maximal value in the voltage range between −40 and +20 mV, where it is nearly voltage independent. At voltages outside this range, the steady-state conductance decreases in a strongly voltage-dependent manner. $G_{H,\ cx50}$ declined asymmetrically for positive and negative voltages. Fitting the mean $G_{hemi} - V_m$ curves with Boltzmann functions shows quantitatively that cx50 hemichannels were much more sensitive to positive potentials with $A = 0.66$, $V_0 = 27$ mV, and $g_{min} = 0.36$ than to negative potentials with $A = 0.05$, $V_0 = -78$ mV, and $g_{min} = 0$. Cx50 hemichannel currents inactivate completely at very large negative potentials, but a large, voltage-independent residual conductance remains after deactivation at any positive voltage. Another major difference between cx46 and cx50 hemichannels is that the steady-state activation curve and the rates of current inactivation of cx50 hemichannels at negative potentials are weakly if at all dependent on $[Ca^{2+}]_{out}$ (data not shown), whereas those of cx46 are strongly dependent on $[Ca^{2+}]_{out}$ (Ebihara and Steiner, 1993).

Voltage-dependent gating properties

The voltage-dependent properties of gap junction channels between teleost horizontal cells can be predicted from the voltage dependent properties of a putative hemichannel current found in the same cells (DeVries and Schwartz, 1992). The voltage dependence and the activation/deactivation kinetics of cx46 and cx56 hemichannel currents at negative voltages predict the behavior of their respective gap junction channels (Ebihara et al., 1995). These studies suggested that cx46 gap junction channels close with relative negativity. Unfortunately, only the negative voltage gate of cx46 hemichannels is seen in macroscopic current recordings. Any voltage-dependent closure of cx46 hemichannels at positive potentials is outside of the experimental range, leaving the possibility that both positive and negative voltage gates share similar dependence on voltage. Indeed, other studies have suggested that cx46 gap junction channels gate with positive polarity based on their response in heterotypic pairings with cx26 (White et al., 1995) and on single channel records of cx46 hemichannels (Trexler et al., 1996). In the latter case, gating polarity of cx46 gap junctions was deduced from the residual conductance state seen in gap junction channels and cx46 single hemichannels. The normalized *G-V* relationship for gap junction channels usually possesses a minimum residual conductance suggesting that gap junction channels close to a subconductance state rather than a fully closed state. Single channel records of gap junctions between an insect cell line reveal transitions between an open state and a subconductance state. Because single cx46 hemichannels enter a subconductance state at positive potentials only, cx46 gap junctional gating was assigned a positive polarity (Trexler et al., 1996).

Fig. 5 shows that the positive gate of cx50 hemichannels, but not the negative gate, has the requisite sensitivity to account for the current-voltage curve of cx50 gap junctions. One way of looking at this is to consider the G_j-V_j relationship in terms of the apparent gating charge, or charge-distance product. For cx50 gap junction channels the charge-distance product is 8.5. Here distance is the fractional distance downfield that the gating charge moves. However, assuming that only one of the two hemichannels that comprise a gap junction channel is actually gating, then the gating charges would move down one-half as much field for the same geometric distance in a junctional channel as they would in a hemichannel. Hence, a charge-distance product of 8.5 for gap junction channels would be equivalent to a twofold greater charge-distance product in hemichannels (i.e., 17). The measured effective charge-distance product of cx50 hemichannels is 16.4 for channel gating at positive potentials, very close to the value of 17 predicted by the junctional value. In contrast, the charge-distance product of the negative voltage gate of cx50 hemichannel is only ~1.3, far too small to account for the steepness of the junctional *G-V* curve.

The residual conductance for cx50 hemichannels (indicating incomplete closure) is present only at positive potentials and is most likely responsible for the residual conductance of cx50 gap junctions, further evidence that cx50 gap junctions close on the relative positive side of the transjunctional potential. If we assume that gap junction channel gating is represented by only one of the hemichannels gating to a subconductance state, then the residual conductance of a gap junction channel composed of two hemichannel conductors in series would be approximately equal to $(G_{hemi,open} \times G_{hemi,closed})/(G_{hemi,open} + G_{hemi,closed})$. Using the residual conductance of cx50 hemichannels at positive potentials, we would predict that cx50 gap junction channels would have a normalized residual conductance smaller than the normalized residual conductance of hemichannels. The residual conductance of cx50 hemichannels at positive voltages is 0.36 of G_{max}. This predicts that the residual conductance of a cx50 gap junction channel would be 0.36 $G_{max}/(1 + 0.36) = 0.26\ G_{max}$. The measured value is 0.21, in good agreement with the predicted value and arguing again that cx50 gap junction channels close on the relative positive side of a transjunctional potential. Cx46 gap junctions have also been assigned relative positive gating based on single channel hemichannel records that show a subconductance state at positive but not negative voltages (Trexler et al., 1996).

In summary, both the voltage sensitivity and residual conductance of cx50 hemichannels at positive potentials predicts the G_j-V_j relationship of cx50 homotypic gap junction channels. Taken together, these data strongly argue that cx50 gap-junctional gating occurs by the gating of a single hemichannel on the relative positive side of a transjunctional potential.

The V_0 of cx50 gap junction channels is lower than expected if we assume that voltage drops equally across each hemichannel and if the gating properties of gap junction channels result from the gating of only one of the component hemichannels. It appears that the *G-V* relationship of cx50 hemichannels shifts to lower voltages when the channels are part of a gap junction channel. Heterotypic gap junction channels display unique gating properties confirming that the voltage dependent behavior of a hemichannel can be modified by interaction with an opposing hemichannel (Barrio et al., 1991; White et al., 1994a). Based on a comparison of cx50 hemichannels and cx50 gap junctional channels, alteration of hemichannel gating properties in the junctional setting is not limited to heterotypic pairings but can occur even in homotypic pairings. A shift in V_0 corresponds to a change in the energy difference between the closed and open states of the channel, a difference that might well arise because of differences in the constraints on the protein imposed by the junctional form. The apparent charge-distant product evident in the voltage dependence of channel closure would be less likely to change in going

from the hemichannel to the junctional environment if the mechanism of gating remained the same.

There is tremendous asymmetry in the properties of the positive and negative voltage gates of cx50 hemichannels, which are clearly resolvable from macroscopic currents. The properties of the positive hemichannel gate resemble the properties of cx50 gap junction behavior, thereby allowing a positive gating polarity to be assigned to cx50 gap junction channels, an assignment that cannot be made so unambiguously for cx46. This assignment of positive relative gating polarity depends on two assumptions. First the gate whose properties are observed in cx50 junctional gating is in fact one of the gates seen in the hemichannel I-V curve. Second the properties of this gate are not much changed in the junction from their properties in the hemichannel. At present there is no way to test these assumptions, but if they are correct, it should be possible to determine if the second hemichannel gate, the negative gating polarity gate, remains functional but normally unobserved in the junctional conformation. The measured hemichannel characteristics suggest that it should be possible to close the negative polarity gate in the junctional conformation at approximately four times the voltage required to close it in the hemichannel conformation, assuming the opposed positive gate remains closed. That is at a voltage of ~200 mV. Oocytes do not tolerate this magnitude of voltage for long. But there is a second possibility that suggests that the effects of the second gate might be detectable at lower potentials, perhaps as low as 80 mV. When a single gate is closed, the voltage will drop mostly across that gate. Although, when the relatively positive gate is closed in the hemichannel configuration, there is still a residual conductance of ~0.3 G_{max}. Thus, ~25% of the voltage would drop across the open negative gate in the junctional configuration. However, the negative gate in the hemichannel configuration closes almost completely. Thus, in the junctional configuration, if both the negative gate and the junctional gate were closed, most of the applied voltage would drop across the negative gate, which would then be more likely to stay closed, in a sense capturing the closed state from the more sensitive opposed positive gate (Bukauskas et al., 2000). This should be detectable macroscopically as a dependence of the time constant of recovery from closure at a fixed potential on the voltage, which produced the closure originally.

Ca^{2+} sensitivity and proton block of Cx50 hemichannels

Cx50 hemichannel currents showed the same sensitivity to external Ca^{2+} as cx46 hemichannel currents. The $pK_{Ca}{}^{2+}$ is ~200 μM for both cx50 and cx46 as well as for cx38. Thus most hemichannel currents seem to be affected by calcium with approximately the same affinity. Our data are the first to provide a comparison between the conductance as a function of Ca^{2+} for cx50 and cx46. This is important because Ca^{2+} shifts the cx46 I-V curve but not the cx50 I-V curve.

Cx50 hemichannels are much more sensitive to external pH than are cx46 hemichannels. The mechanism by which protons affect the magnitude of hemichannel current is unknown. Most gap junction channels close upon cytoplasmic acidification. Gap junctions composed of cx43 are blocked by cytoplasmic acidification via a ball-and-chain mechanism involving H95 (Dunham et al., 1992; Liu et al., 1993; Ek et al., 1994; Morley et al., 1996). Both cx46 and cx50 gap junction channels are sensitive to cytoplasmic acidification, but the mechanism of block is unknown (White et al., 1994b).

One could argue that protons enter the cytoplasm through open hemichannels and subsequently block hemichannel current by the same mechanism responsible for the cytoplasmic acidification induced closure of gap junction channels. Zampighi et al. (1999) have shown that cytoplasmic acidification of oocytes with sodium acetate blocks cx50 hemichannels. It is difficult to say if the same mechanisms are acting in these two cases. Our results (Fig. 6) provide the only titration curve available for cx50 hemichannels. We found a much higher pK for cx50 hemichannel inactivation than Trexler et al. (1996) found for cx46 hemichannels (7.42 for cx50, 6.4) and our titration curve has a rather small apparent Hill coefficient (0.62) compared with a rather steep one (2.3) for cx46. We were unable to determine if the two histidines in the third transmembrane domain of cx50 play any role in hemichannel pH sensitivity, in the case of one mutant because it killed the oocytes before sufficiently detailed measurements could be made and in the case of the other because it does not form hemichannels.

Mutants

Due to the possible importance of pH in lens physiology (Nemeth-Cahalan and Hall, 2000), the pH dependence of cx50 hemichannels was further explored by biochemical modification and mutational analysis of histidine residues. Modification of histidine residues exposed to the external environment by DEPC completely eliminates cx50 hemichannel current but not cx46 hemichannel current. DEPC-modified histidines could act by blocking the channel pore or by affecting the hemichannel voltage gate to prevent channel openings. Mutational analysis of two different histidine residues unique to cx50 and located in the presumptive third transmembrane a domain produced interesting effects but did not directly demonstrate a role for these residues in conferring pH sensitivity on cx50 hemichannels. We should emphasize once again that this is not because these residues do not participate in pH control of hemichannel conductance but

simply because it is impossible to study the properties of these mutant hemichannels in detail.

The H161N mutation abolished hemichannel current activity without affecting gap junction formation or the voltage dependence of junctional conductance. We have already seen from the cx50 $G_h - V_m$ curve that there are two voltage-dependent gates present in hemichannels. One gate that operates in both hemichannels and gap junction channels (the junctional gate, which has steeper voltage dependence), and a second less voltage dependent gate operates only in hemichannels mode. The H161N mutation may alter one of the hemichannel gates so that it is permanently closed or it may prevent hemichannel opening by some other means. But it does not alter junctional gating. The fact that the presence of the N residue in the corresponding position of cx46 does not prevent cx46 from forming hemichannels suggests two things: first that the H161N mutation does dramatically close the hemichannel gate and second that regions of the cx46 molecule quite distinct from the position of residue 161 make up an important part of the hemichannel gate.

The H176Q mutation resulted in lysis of the oocytes. Normally, over-expression of functional hemichannels will eventually cause lysis due to a steady increase in whole-cell conductance and lysis is easily prevented by incubating oocytes in osmotically buffered media or by increasing the concentration of external divalent cations to keep hemichannels closed (Ebihara and Steiner, 1993). However, increasing $[Ca^{2+}]_{out}$ or decreasing pH_{out} does not prevent lysis of oocytes expressing the H176Q mutation. Furthermore, oocytes expressing H176Q develop unique disturbances in the pigmentation pattern that are not accompanied by a depolarization of the resting potential. This suggests that the events leading to lysis are different for H176Q than they are for other hemichannel forming connexins. The lethal phenotype of cx50H176Q can be rescued by co-expression of wild-type cx50 and possibly as few as one single wild-type subunit in one hemichannel (or connexon) is sufficient.

The H176Q mutation is positioned in an interesting place in the cx50 sequence. In one model of the hemichannel pore, a region of sequence between the presumptive third transmembrane domain and the second extracellular loop is proposed to move in and out of the plasma membrane much like the P-loop of voltage gated sodium channels (Dahl et al., 1994). One possibility is that this region must be inserted into the plasma membrane to produce a functional channel. In connexins that do not form functional hemichannels, this region extends out into the extracellular space and interaction with an opposing hemichannel moves this region into the plasma membrane. In connexins that form functional hemichannels, this region can insert itself into the plasma membrane without interacting with an opposing hemichannel. Possibly the ionized form of histidine displaces this region out of the plasma membrane, resulting in the closure of the hemichannel. When this histidine is missing, the segment remains in the membrane and the hemichannel remains functional. Because the voltage-dependent properties of cx50 keep the hemichannel open at normal resting potentials, there must be a way to keep the hemichannel from opening during trafficking to the plasma membrane. H176 may play this role possibly explaining why replacing it with an uncharged amino acid kills the oocytes.

Alternatively, a charge interaction between ionized histidine and a nearby acidic residue could keep the hemichannel closed at low pH. One possible candidate is cx50D3. This interpretation is strengthened by the observation that a cataract causing mutant cx50D3A (JF1) exhibits the H176Q phenotype when expressed in oocytes (data not shown). The N-terminal sequence of connexin polypeptides is resistant to proteolytic cleavage, suggesting it is buried in the plasma membrane, the interior of the protein, or the channel pore (Milks et al., 1988). The identical behavior of cx50 H176N and cx50D3A suggests a possible interaction between the H176 and D3 residues. Perhaps a salt bridge forms at low pH to prevent hemichannel openings during trafficking to the plasma membrane. Activity of hemichannels in trafficking vesicles will change the ionic composition of these compartments and may result in the failure to express any membrane resident protein, including those required to maintain oocyte viability. The double mutant, cx50/H61N/H176Q did not result in functional hemichannels probably due to a dominant negative affect of H161N, but remains to be assayed as to how gap junction properties are altered.

Relevance to lens physiology

Hemichannels may play a role distinct from gap junctional communication. The functional significance of hemichannel activity in lens tissue has been ruled unlikely due to the apparent high impedance of lens fiber cell membranes (Mathias et al., 1979). However, whole-cell currents resembling cx46 and cx50 hemichannel currents have been found in peripheral fiber cells isolated in low calcium containing solutions (Eckert et al., 1998). Functional hemichannels must now be included as candidates for the unidentified channels responsible for the Na^+ and K^+ leak conductances of fiber cells.

Our studies show that the two connexins expressed in lens fiber cells form hemichannels with different voltage-dependence and sensitivity to external pH. The whole-cell conductance of cx50 is maximal at typical resting potentials (-40 mV) and is most sensitive to external calcium and pH in a voltage independent manner. Conversely, steady-state cx46 hemichannel conductance is most sensitive to external calcium and membrane potential.

As we approach the center of the lens, the resting potentials decrease from -60 mV to -20 mV, and the environ-

ment becomes more acidic. At any given external calcium concentration, the steady-state current through cx46 hemichannels would increase as we move toward the center of the lens due to more depolarized membrane potentials (Mathias and Rae, 1985). The increased cx46 hemichannel conductance, however, would be offset by the pH-dependent decrease in cx50 hemichannel conductance that would occur in the more acidic interior of the lens. Hence, differences in the voltage dependence and pH sensitivity of hemichannels formed by the two fiber cell connexins, cx46 and cx50, could provide for homeostatic regulation of total lens current. The regulation would be exerted at the interface between fiber cell membrane and the interstitial space, where hemichannel activity could mediate the entry of Na^+ into fiber cells. Changes in external calcium would adjust the magnitude of the combined total current flowing into fiber cells. This is a fundamentally different role than regulating gap junctional coupling between fiber cells. Only future experiments can determine if hemichannels actually play any role at all in normal lens physiology. Certainly, as required by the impedance studies of Mathias et al. (1985, 1997; Mathias and Rae, 1985) only a very few hemichannels per fiber cell could be open at any given time.

We would like to thank Mary Hawley and Tiba Ayenichi for expert technical assistance. This work was supported by National Institutes of Health Grant EY 05661 (to J.E.H.).

REFERENCES

Barrio, L. C., T. Suchyna, T. A. Bargiello, L. X. Xu, R. S. Roginshi, M. V. L. Bennett, and B. J. Nicholson. 1991. Gap junctions formed by connexins 26 and 32 alone and in combination are differently affected by applied voltage. *Proc. Natl. Acad. Sci. U. S. A.* 88:8410–8414.

Bassnett, S., and G. Duncan. 1988. The influence of pH on membrane conductance and intercellular resistance in the rat lens. *J. Physiol. (Lond.)* 398:507–521.

Bruzzone, R., J. A. Haefliger, R. L. Gimlich, and D. L. Paul. 1993. Connexin40, a component of gap junctions in vascular endothelium, is restricted in its ability to interact with other connexins. *Mol. Biol. Cell.* 4:7–20.

Bukauskas, F. F., K. Jordan, A. Bukauskiene, M. V. Bennett, P. D. Lampe, D. W. Laird, and V. K. Verselis. 2000. Clustering of connexin 43-enhanced green fluorescent protein gap junction channels and functional coupling in living cells. *Proc. Natl. Acad. Sci. U. S. A.* 97:2556–2561.

Dahl, G., W. Nonner, and R. Werner. 1994. Attempts to define functional domains of gap junction proteins with synthetic peptides. *Biophys. J.* 67:1816–1822.

DeVries, S. H., and E. A. Schwartz. 1992. Hemi-gap-junction channels in solitary horizontal cells of the catfish retina. *J. Physiol. (Lond.)* 445: 201–230.

Dunham, B., S. Liu, S. Taffet, E. Trabka-Janik, M. Delmar, R. Petryshyn, S. Zheng, R. Perzova, and M. L. Vallano. 1992. Immunolocalization and expression of functional and nonfunctional cell-to-cell channels from wild-type and mutant rat heart connexin43 cDNA. *Circ. Res.* 70: 1233–1243.

Ebihara, L., V. M. Berthoud, and E. C. Beyer. 1995. Distinct behavior of connexin56 and connexin46 gap junctional channels can be predicted from the behavior of their hemi-gap- junctional channels. *Biophys. J.* 68:1796–1803.

Ebihara, L. and E. Steiner. 1993. Properties of a nonjunctional current expressed from a rat connexin46 cDNA in *Xenopus* oocytes. *J. Gen. Physiol.* 102:59–74.

Eckert, R., P. Donaldson, K. Goldie, and J. Kistler. 1998. A distinct membrane current in rat lens fiber cells isolated under calcium-free conditions. *Invest. Ophthalmol. Vis. Sci.* 39:1280–1285.

Ek, J. F., M. Delmar, R. Perzova, and S. M. Taffet. 1994. Role of histidine 95 on pH gating of the cardiac gap junction protein connexin43. *Circ. Res.* 74:1058–1064.

Gong, X., E. Li, G. Klier, Q. Huang, Y. Wu, H. Lei, N. M. Kumar, J. Horwitz, and N. B. Gilula. 1997. Disruption of α3 connexin gene leads to proteolysis and cataractogenesis in mice. *Cell.* 91:833–843.

Goodenough, D. A., D. L. Paul, and L. Jesaitis. 1988. Topological distribution of two connexin32 antigenic sites in intact and split rodent hepatocyte gap junctions. *J. Cell Biol.* 107:1817–1824.

Gupta, V. K., V. M. Berthoud, N. Atal, J. A. Jarillo, L. C. Barrio, and E. C. Beyer. 1994. Bovine connexin44, a lens gap junction protein: molecular cloning, immunologic characterization, and functional expression. *Invest. Ophthalmol. Vis. Sci.* 35:3747–3758.

Hennemann, H., T. Suchyna, H. Lichtenberg-Frate, S. Jungbluth, E. Dahl, J. Schwarz, B. J. Nicholson, and K. Willecke. 1992. Molecular cloning and functional expression of mouse connexin40, a second gap junction gene preferentially expressed in lung. *J. Cell Biol.* 117:1299–1310.

Hille, B. 1992. Ionic Channels of Excitable Membranes. Sinauer Associates Inc., Sunderland, MA.

Jedamzik, B., I. Marten, A. Ngezahayo, A. Ernst, and H. A. Kolb. 2000. Regulation of lens rCx46-formed hemichannels by activation of protein kinase C, external Ca(2+) and protons. *J. Membr. Biol.* 173:39–46.

Jongsma, H. J., R. Wilders, A. C. G. Van Ginneken, and M. B. Rook. 1991. Modulatory effect of the transcellular electrical field on gap junction conductance. *In* Biophysics of Gap Junction Channels. C. Peracchia, editor. CRC Press, Inc., Boca Raton, FL. 163–172.

Laird, D. W., and J. P. Revel. 1990. Biochemical and immunochemical analysis of the arrangement of connexin43 in rat heart gap junction membranes. *J. Cell Sci.* 97:109–117.

Liu, S., S. Taffet, L. Stoner, M. Delmar, M. L. Vallano, and J. Jalife. 1993. A structural basis for the unequal sensitivity of the major cardiac and liver gap junctions to intracellular acidification: the carboxyl tail length. *Biophys. J.* 64:1422–1433.

Mathias, R. T., and J. L. Rae. 1985. Steady state voltages in the frog lens. *Curr. Eye Res.* 4:421–430.

Mathias, R. T., J. L. Rae, and G. J. Baldo. 1997. Physiological properties of the normal lens. *Physiol. Rev.* 77:21–50.

Mathias, R. T., J. L. Rae, L. Ebihara, and R. T. McCarthy. 1985. The localization of transport properties in the frog lens. *Biophys. J.* 48: 423–434.

Mathias, R. T., J. L. Rae, and R. S. Eisenberg. 1979. Electrical properties of structural components of the crystalline lens. *Biophys. J.* 25:181–201.

Mathias, R. T., G. Riquelme, and J. L. Rae. 1991. Cell to cell communication and pH in the frog lens. *J. Gen. Physiol.* 98:1085–1103.

Miles, E. W. 1977. Modification of histidyl residues in proteins by diethylpyrocarbonate. *Methods Enzymol.* 47:431–442.

Milks, L. C., N. M. Kumar, R. Houghten, P. N. Unwin, and N. B. Gilula. 1988. Topology of the 32-kd liver gap junction protein determined by site-directed antibody localizations. *EMBO J.* 7:2967–2975.

Miller, A. G., C. Y. Chan, and J. E. Hall. 1992. Effects of pH on junctional permeability in dissociated embryonic chicken lens cells. *Biophys. J.* 61:507.

Morley, G. E., S. M. Taffet, and M. Delmar. 1996. Intramolecular interactions mediate pH regulation of connexin43 channels. *Biophys. J.* 70:1294–1302.

Nemeth-Cahalan, K. L., and J. E. Hall. 2000. pH and calcium regulate the water permeability of aquaporin 0. *J. Biol. Chem.* 275:6777–6782.

Padan, E., L. Patel, and H. R. Kaback. 1979. Effect of diethylpyrocarbonate on lactose/proton symport in *Escherichia coli* membrane vesicles. *Proc. Natl. Acad. Sci. U. S. A.* 76:6221–6225.

Pasquale, L. R., R. T. Mathias, L. R. Austin, P. R. Brink, and M. Ciunga. 1990. Electrostatic properties of fiber cell membranes from the frog lens. *Biophys. J.* 58:939–945.

Paul, D. L., L. Ebihara, L. J. Takemoto, K. I. Swenson, and D. A. Goodenough. 1991. Connexin46, a novel lens gap junction protein, induces voltage-gated currents in nonjunctional plasma membrane of *Xenopus* oocytes. *J. Cell Biol.* 115:1077–1089.

Pfahnl, A., and G. Dahl. 1998. Localization of a voltage gate in connexin46 gap junction hemichannels. *Biophys. J.* 75:2323–2331.

Pfahnl, A., and G. Dahl. 1999. Gating of cx46 gap junction hemichannels by calcium and voltage. *Pflugers Arch.* 437:345–353.

Rai, S. S., and J. Wolff. 1998. Localization of critical histidyl residues required for vinblastine-induced tubulin polymerization and for microtubule assembly. *J. Biol. Chem.* 273:31131–31137.

Shoshan-Barmatz, V., and S. Weil. 1994. Diethyl pyrocarbonate modification of the ryanodine receptor/Ca^{2+} channel from skeletal muscle. *Biochem. J.* 299:177–181.

Spires, S., and T. Begenisich. 1990. Modification of potassium channel kinetics by histidine-specific reagents. *J. Gen. Physiol.* 96:757–775.

Trexler, E. B., M. V. Bennett, T. A. Bargiello, and V. K. Verselis. 1996a. Voltage gating and permeation in a gap junction hemichannel. *Proc. Natl. Acad. Sci. U. S. A.* 93:5836–5841.

White, T. W., R. Bruzzone, D. A. Goodenough, and D. L. Paul. 1994a. Voltage gating of connexins. *Nature.* 371:208–209.

White, T. W., R. Bruzzone, S. Wolfram, D. L. Paul, and D. A. Goodenough. 1994b. Selective interactions among the multiple connexin proteins expressed in the vertebrate lens: the second extracellular domain is a determinant of compatibility between connexins. *J. Cell Biol.* 125:879–892.

White, T. W., D. A. Goodenough, and D. L. Paul. 1998. Targeted ablation of connexin50 in mice results in microphthalmia and zonular pulverulent cataracts. *J. Cell Biol.* 143:815–825.

White, T. W., D. L. Paul, D. A. Goodenough, and R. Bruzzone. 1995. Functional analysis of selective interactions among rodent connexins. *Mol. Biol. Cell.* 6:459–470.

Wilders, R., and H. J. Jongsma. 1992. Limitations of the dual voltage clamp method in assaying conductance and kinetics of gap junction channels. *Biophys. J.* 63:942–953.

Yeager, M., and N. B. Gilula. 1992. Membrane topology and quaternary structure of cardiac gap junction ion channels. *J. Mol. Biol.* 223: 929–948.

Zampighi, G. A., D. D. Loo, M. Kreman, S. Eskandari, and E. M. Wright. 1999. Functional and morphological correlates of connexin50 expressed in *Xenopus laevis* oocytes. *J. Gen. Physiol.* 113:507–524.